ACS APPLIED MATERIALS & INTERFACES

Research Article

Cite This: ACS Appl. Mater. Interfaces XXXX, XXX, XXX−XXX

www.acsami.org

Novel High-Energy-Density Rechargeable Hybrid Sodium−Air Cell with Acidic Electrolyte

Yao Kang,[†,▽] Fengmei Su,[†,▽] Qingkai Zhang,[†] Feng Liang,[*,†,‡] Keegan R. Adair,[§] Kunfeng Chen,[∥] Dongfeng Xue,[∥] Katsuro Hayashi,[⊥] Shan Cecilia Cao,[#] Hossein Yadegari,[§] and Xueliang Sun[§]

[†]Faculty of Metallurgical and Energy Engineering and [‡]State Key Laboratory of Complex Nonferrous Metal Resources Clean Utilization, Kunming University of Science and Technology, Kunming 650093, China

[§]Department of Mechanical and Materials Engineering, University of Western Ontario, London, Ontario N6A 5B9, Canada

[∥]State Key Laboratory of Rare Earth Resources Utilization, Chinese Academy of Sciences, Changchun 130022, China

[⊥]Department of Applied Chemistry, Faculty of Engineering, Kyushu University, Fukuoka 819-0395, Japan

[#]Department of Material Science and Engineering, Massachusetts Institute of Technology, Cambridge, Massachusetts 02139, United States

Supporting Information

ABSTRACT: Low-cost, high-energy-density, and highly efficient devices for energy storage have long been desired in our society. Herein, a novel high-energy-density hybrid sodium−air cell was fabricated successfully on the basis of acidic catholytes. Such a hybrid sodium−air cell possess a high theoretical voltage of 3.94 V, capacity of 1121 mAh g^{-1}, and energy density of 4418 Wh kg^{-1}. First, the buffering effect of an acidic solution was demonstrated, which provides relatively long and stable cell discharge behaviors. Second, the catholytes of hybrid sodium−air cells were optimized systematically from the solutions of 0.1 M H_3PO_4 + 0.1 M Na_2SO_4 to 0.1 M HAc + 0.1 M NaAc and it was found that the cells with 0.1 M H_3PO_4 + 0.1 M Na_2SO_4 displayed a maximum power density of 34.9 mW cm^{-2}. The cell with 0.1 M H_3PO_4 + 0.1 M Na_2SO_4 displayed higher discharge capacity of 896 mAh g^{-1}. Moreover, the fabricated acidic hybrid sodium−air cells exhibited stable cycling performance in ambient air and they delivered a low voltage gap around 0.3 V when the current density is 0.13 mA cm^{-2}, leading to a high energy efficiency up to 90%. Therefore, the present study provides new opportunities to develop highly cost-effective energy storage technologies.

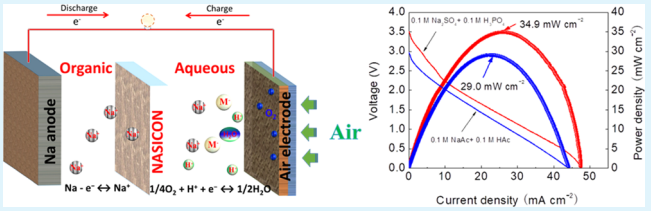

KEYWORDS: *sodium−air cell, electrolyte, phosphoric acid, acetic acid, electrochemical performance*

INTRODUCTION

The growing energy needs and environment concerns motivate us to design highly effective electrical energy storage systems (EESS). Metallic sodium has been widely studied to construct high-energy-density energy storage because of the large abundance of sodium compared to lithium, which enables the sustainable development of energy storage technology.[1−4] In addition, sodium is a light metal with a low reduction potential, which contributes to its high energy density.[1−4] Among various sodium-based energy systems (Na-ion, Na−S batteries), Na−air cells are the most promising EESS to solve the energy crisis.[4−10]

Scientists have focused on nonaqueous sodium−air batteries for many years, and significant efforts have been reported to improve cell performances.[11−15] The insoluble discharge products (e.g., NaO_2 and Na_2O_2) during discharge process lead to the gradual accumulation of products and blocking of the porous air electrode, thus resulting in battery deterioration after long time of working.[11−13] Therefore, the nonaqueous sodium−air cells have significant practical energy and capacity limitations. In addition, the large overpotential observed in nonaqueous sodium−air cells results in a low round-trip efficiency, which greatly decreases electrochemical performance of batteries.[14,15] Therefore, to enhance the performance of these batteries, a new hybrid sodium−air cell was proposed by utilizing NASICON solid electrolyte to protect the sodium anode.[8,9] Because of the single sodium-ion conducting nature of the NASICON and its ability to block contaminants from the air, the hybrid sodium−air cell has shown excellent potential as a next-generation electrochemical energy storage device.[16−18]

Up until now, the common use of supporting salt (NaOH) not only provides the basic condition to enhance the oxygen reduction reaction (ORR) but also increases conductivity of the aqueous electrolyte by providing Na^+.[16−1816−18] The reaction is as follows

Hybrid:

$$Na + 1/4O_{2(g)} + 1/2H_2O_{(l)} \leftrightarrow NaOH_{(l)} \quad (1)$$

Received: March 15, 2018
Accepted: June 22, 2018
Published: June 22, 2018

DOI: 10.1021/acsami.8b04278
ACS Appl. Mater. Interfaces XXXX, XXX, XXX−XXX

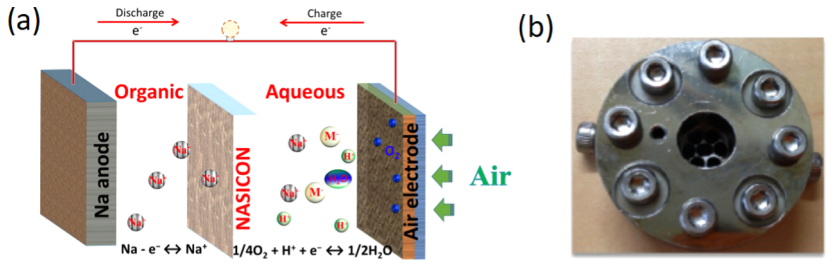

Figure 1. (a) Schematic illustration of a typical hybrid sodium−air cell. (b) The photo of practical hybrid sodium−air battery.

Table 1. Reactions, Standard Voltages, Energy Densities, and Capacities of Two Kinds of Hybrid Sodium−Air Cells

system	reaction	standard voltage (V)	energy density (Wh kg^{-1})	capacity (mAh g^{-1})
Na−alkaline	$Na + 1/4O_2 + 1/2H_2O \leftrightarrow Na^+ + OH^-$	3.11	2600	838
Na−acidic	$Na + 1/4O_2 + H^+ \leftrightarrow Na^+ + 1/2H_2O$	3.94	4418	1121.4

In addition, a fantastic theoretical voltage (3.11 V), specific capacity (2600 Wh kg^{-1}), and low discharge voltage gap was obtained in hybrid Na−air cells by using basic solution compared to nonaqueous sodium−air cells.[8,9,19−21] However, hybrid Na−air cell still faces some significant challenges when NaOH is selected as the supporting salt. First, a high concentration of Na^+ can improve the conductivity of the aqueous electrolyte while it also leads to high alkalinity that lowers the solubility of oxygen in aqueous electrolyte.[8,9,22,23] However, the discharge voltage increases with the decrement concentration of NaOH due to the higher solubility of oxygen in lower alkaline concentration.[8,22] Second, NaOH is utilized during long-term working, which leads to a sharp decrease in NaOH concentration and an increase in the internal resistance, exhibiting larger voltage hysteresis.[4,9,22] Most importantly, the electrochemical performances of alkaline-based hybrid sodium−air cells decrease because of the side reactions caused by carbon dioxide. It is well known that Li_2CO_3 is not reversible in hybrid lithium−air cells; the irreversible product of Na_2CO_3 also occurred in alkaline-based hybrid sodium−air cells due to the similar structure and working mechanisms between hybrid sodium−air and lithium−air cells.[24] Therefore, hybrid sodium−air cells using acidic electrolyte were proposed with additional supporting salts to enhance ionic conductivity of catholyte. Furthermore, an appropriate pH value should be considered to ensure the stability of the catholyte. Recently, a hybrid Na−air flow cell using an acidic catholyte with a maximum power density of 5.5 mW cm^{-2} was reported by Kim et al.; however, the power density is still far from that required for application in electric vehicles.[25] In addition, the effect of acid solutions and supporting salts on the performances of hybrid sodium−air cells is still unclear. It is necessary to select appropriate acids and match supporting salts for the catholyte to improve the electrochemical performances of hybrid Na−air cells.

Herein, we present a hybrid sodium−air cell based on acidic electrolytes, which exhibits good electrochemical performances compared to those of previously reported alkali metal−air cells. Generally, strong acids such as HCl and HNO_3 have slight degradation on NASICON due to the interaction between acid and NASICON; thus, these cannot support stable long-term working of a battery.[26,27] Therefore, to ensure the stability of battery and improve conductivity of catholyte, 0.1 M HAc + 0.1 M NaAc and 0.1 M H_3PO_4 + 0.1 M Na_2SO_4 were utilized as catholyte. The acid in the electrolyte can effectively eliminate the side reactions, and the supporting salts are used to increase ionic conductivity. Therefore, the fabricated hybrid sodium−air cells delivered fantastic electrochemical performances.

Figure 1a shows a typical structure of the hybrid sodium−air cell, which is constructed as follows: Na ‖anolyte‖ NASICON ‖acidic catholyte‖ catalytic air electrode. Figure 1b is the photo of a practical hybrid sodium−air battery. During discharge, oxygen in the air is reduced to H_2O at the catalytic sites of catalyst, while sodium is oxidized to sodium ion and diffuses into the catholyte after passing through the organic electrolyte and NASICON. During the charge process, sodium ion in the aqueous electrolyte is transferred back to the anode side and then it is electrodeposited on the anode substrate. During the discharge−charge process, the half−cell reaction of cathode and anode and their standard potentials are given by eqs 2 and 3. The overall reaction is indicated by eq 4.

Cathode

$$1/4O_2 + H^+ + e^- \leftrightarrow 1/2H_2O, E^\theta = +1.23\ V \quad (2)$$

Anode

$$Na \leftrightarrow Na^+ + e^-,\ E^\theta = -2.71\ V \quad (3)$$

Overall

$$Na + 1/4O_2 + H^+ \leftrightarrow Na^+ + 1/2H_2O, E^\theta = +3.94\ V \quad (4)$$

The standard cell voltage of acid-based hybrid sodium−air cell is 3.94 V, which is much higher than that of alkaline-based hybrid sodium−air cells (3.11 V). Table 1 shows electrochemical reactions, standard voltages, energy densities, and capacities of two kinds of hybrid sodium−air cells.

The theoretical capacity is described by *C*, which is calculated according to the weights of 1 mol sodium and 1 mol H^+.

$$C_{Na-air} = \frac{\text{Faraday constant}}{\text{mass of theoretical active materials}} \times \frac{1000}{3600} = \frac{96\,485}{22.90 + 1} \times \frac{1000}{3600} = 1121.4\ \text{mAh}\ g^{-1} \quad (5)$$

Theoretical energy density was calculated as follows

$$E_{Na-air}{}^* = \text{theoretical capacity} \times \text{standard voltage} = 1121.4\ \text{mAh}\ g^{-1} \times 3.94,\ V = 4418\ \text{Wh}\ kg^{-1} \quad (6)$$

Therefore, the fabricated hybrid sodium−air cell with acidic electrolyte possesses fantastic electrochemical performances;

DOI: 10.1021/acsami.8b04278
ACS Appl. Mater. Interfaces XXXX, XXX, XXX−XXX

especially, because of its energy density, it is superior to lithium−ion batteries and can potentially enable electrical vehicles to travel longer distances per charge.

EXPERIMENTAL SECTION

Preparation of Catalytic Air Electrode. To prepare the air electrode, the catalyst ink was first prepared by sonicating 20 mg of 40 wt % Pt/C (Junji JJ040, China) powder in a mixture of water and ethanol (1:1) (2 mL) with 5 wt % poly(tetrafluoroethylene) (5 μL) as binder. The catalyst ink was then dropped onto carbon paper (Toray 060, Japan) to prepare catalytic electrode with the loading of 1 mg cm^{-2}.

Assembly of the Cells. A Na disk (99.9%) with a 0.3 mm thickness and 1 cm diameter was cut as the anode. An organic liquid electrolyte, 1 M $NaClO_4$ in ethylene carbonate/dimethyl carbonate (1:1 volume ratio) with 1 vol % fluoroethylene carbonate was purchased from Mojiesi Energy Company (China). Solutions of 0.1 M H_3PO_4 (acid solution) + 0.1 M Na_2SO_4 (supporting salt) and 0.1 M HAc (acid solution) + 0.1 M NaAc (supporting salt) were employed as catholytes. A piece of NASICON with the composition of $Na_3Zr_2Si_2PO_{12}$ having a high ionic conductivity of 1.3×10^{-3} S cm^{-1} at room temperature was used as the separator.[4] In our work, the metallic sodium was plated on a stainless steel anode flange equipped with a nitrile rubber O-ring and an organic electrolyte was poured onto it in a glovebox. Then, this anode compartment was hermetically sealed by NASICON, another O-ring, and an insulating flange made of poly(ether ether ketone) resin. Finally, 0.2 mL of the catholyte was dropped on the NASICON and the air electrode was placed on the top.

Electrochemical Performance Test. The assembled Na−air cell was connected to the testing station and tested in the atmospheric air. Charge−discharge performance was measured by a LAND cell tester (CT2001A, Wuhan LAND electronics). PARSTAT 4000 rear panel was used to carry out electrochemical impedance spectroscopy (EIS) measurement. The alternating current perturbation signal of ±10 mV and the frequency range from 0.01 to 50 000 Hz was employed for measurement. Current−voltage and areal power density−voltage characteristics of the cells were measured with a PARSTAT 4000 rear panel using a sweep rate of 0.01 mV s^{-1}. The electrochemical performance of hybrid sodium−air cells was tested at 30 °C with a relative humidity, R_H, of 80%.

Characterization. X-ray diffraction (XRD) (MiniFlex 600, Japan) equipped with Cu Kα radiation was employed for investigating the stability of NASICON separator from 10 to 70° at a scan rate of 0.02° s^{-1}.

RESULTS AND DISCUSSION

The stability of the NASICON solid electrolyte is the key to ensure the electrochemical performance of batteries, especially for their long lifetime. Ideally, the ceramic separator should be compatible in various pH values to accommodate the pH change of aqueous electrolyte during the whole working process. Strong acids are undesirable for a hybrid sodium−air cell due to the slight corrosion of NASICON solid in low pH environments.[26,27] XRD patterns of NASICON plates after immersion in two electrolytes are shown in Figure 2. The NASICON plate was completely decomposed in 0.1 M HCl solution and showed very different diffraction patterns. It has been demonstrated that dissolution of oxides and exchange between H^+ and Na^+ is unavoidable for NASICON when it was working in low pH aqueous condition.[28,29] Therefore, weaker HAc and H_3PO_4 with a support salt were utilized as the catholyte to fabricate hybrid sodium−air cells. On one hand, the supporting salt can enhance ionic conductivity of catholyte, which is of great value to improve the power density of a battery. On the other hand, pure acid is still undesirable due to its low pH value when the stability of NASICON was considered; therefore, supporting salt was introduced to hinder the dissociation of the solid electrolyte and

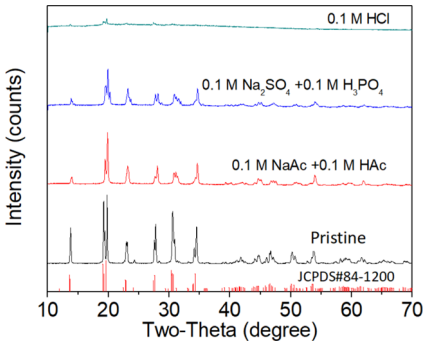

Figure 2. XRD peaks of pristine NASICON plate after immersion in various aqueous solutions of 0.1 M HAc + 0.1 M NaAc, 0.1 M H_3PO_4 + 0.1 M Na_2SO_4, and 0.1 M HCl for 3 days.

increase the pH value of the solution. The XRD pattern of the NASICON plate immersed in 0.1 M HAc + 0.1 M NaAc and 0.1 M H_3PO_4 + 0.1 M Na_2SO_4 aqueous solutions for 3 days showed no extra phase formation compared to that of the pristine NASICON plate, indicating an acceptable stability of the NASICON plate against the acid electrolytes. However, the peak intensity of NASICON slightly changed; this is ascribed to the gentle generation of H_3O^+-type NASICON caused by exchange between protons and Na^+.[29,29] However, the gentle generation of H_3O^+-type NASICON does not cause significant degradation in ionic conductivity. Thus, compared to strong acid catholytes, weaker acids such as HAc or H_3PO_4 can be more promising candidates used in hybrid sodium−air cells.

To investigate the effects of different acids on the cell performances during discharge, weak acids with appropriate concentration of 0.05 M were utilized. As we can see from the discharge curves in Figure 3, the cells displayed two discharge plateaus in 0.05 HAc + 0.1 M NaAc electrolyte. The first voltage plateau corresponds to eq 4, which exhibits a higher discharge voltage compared to that of the second plateau. Since one proton is released from HAc and consumed after a long

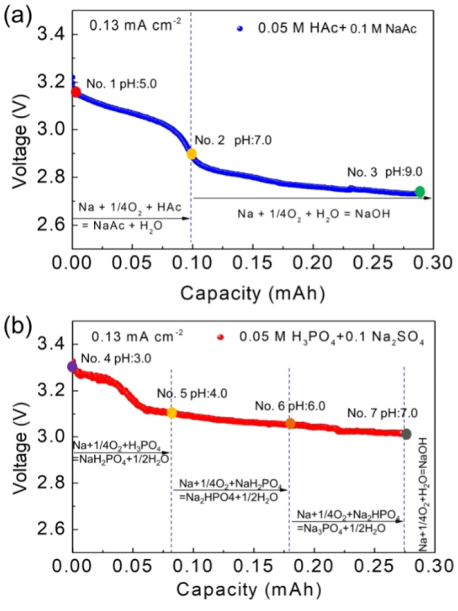

Figure 3. Discharge curves of hybrid sodium−air cell with 0.05 M acid solution: (a) 0.05 M HAc + 0.1 M NaAc and (b) 0.05 M H_3PO_4 + 0.1 M Na_2SO_4.

DOI: 10.1021/acsami.8b04278
ACS Appl. Mater. Interfaces XXXX, XXX, XXX−XXX

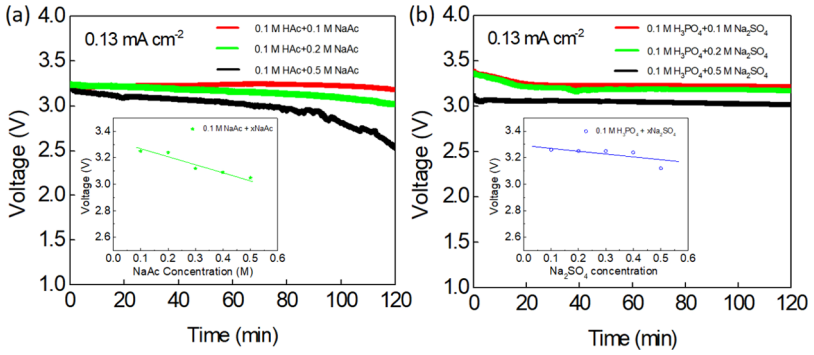

Figure 4. Discharge profiles of hybrid sodium−air cell with different aqueous electrolytes: (a) different concentrations of support salt in 0.1 M HAc; (b) different concentrations of support salt in 0.1 M H_3PO_4. Inset is the supporting salt concentration dependence of discharge voltage in a hybrid sodium−air battery.

operation, it results in a sharp decrease of discharge voltage.[26,27] This result can be explained by eq 1, which possesses a lower standard voltage compared to that in eq 4. Correspondingly, to illustrate the reaction mechanisms of cells during different stages of discharge, pH values of the catholytes were measured by pH paper at the end of each discharge stage. The pH values measured at different states of discharge are denoted by numbers, as seen in Figure 3. For the cell containing a 0.05 M HAc + 0.1 M NaAc catholyte, the initial discharge step has a pH value of around 5.0 (no. 1), which is ascribed to the eq 4, where no OH^- is generated. In stage no. 2, the pH value decreases to 7.0, which is mainly due to the consumption of protons. At the end of the discharge, the pH value of catholyte rapidly increased to 9.0 (no. 3), indicating the generation and accumulation of OH^-. Different discharge behaviors can be found in the hybrid sodium−air cell with 0.05 M H_3PO_4 + 0.1 M Na_2SO_4 acid electrolyte. Figure 3b shows a more stable discharge curve; the cell voltage demonstrates a slow decrement at the end of discharge due to the buffering effect of acid. The mechanism of the catholyte containing 0.05 M H_3PO_4 + 0.1 M Na_2SO_4 corresponds to the following three-step reaction

$$Na + H_3PO_4 + 1/4O_2 = NaH_2PO_4 + 1/2H_2O \quad (7)$$

$$Na + NaH_2PO_4 + 1/4O_2 = Na_2HPO_4 + 1/2H_2O \quad (8)$$

$$Na + Na_2HPO_4 + 1/4O_2 = Na_3PO_4 + 1/4H_2O \quad (9)$$

As soon as the discharge process begins, H_3PO_4 is consumed and $(H_2PO_4)^-$ is produced (no. 4: pH = 3.0). The solution becomes a buffer including H_3PO_4 and its conjugate base $(H_2PO_4)^-$, which is the first buffer zone. As the discharge process continues, $(H_2PO_4)^-$ is consumed and $(HPO_4)^{2-}$ is produced and acts as a second buffer zone. Furthermore, the pH value experienced a sharp rise from 4.0 (no. 5) to 6.0 (no. 6) due to the large difference of dissociation constants. Upon further discharge, the pH value is observed to increase slightly after the second equivalency point (no. 6), which can be explained by the balance of dissociation and ionization of Na_3PO_4. In the third buffer zone, $(HPO_4)^{2-}$ and its conjugate base $(PO_4)^{3-}$ are left in the catholyte. It is the hydrolysis of Na_3PO_4 that contributes to the alkalinity of Na_3PO_4 in the solution (pH = 6.0). Although the cell with 0.05 M H_3PO_4 + 0.1 M Na_2SO_4 indicates a relatively more stable and flat discharge curve due to its buffering effect, it is notable that lower concentrations of acids are not a good choice due to the limited capacity.

Appropriate 0.1 M HAc and 0.1 M H_3PO_4 acidic solutions were used to ensure the stability and discharge behaviors of the cells. Correspondingly, the same concentration of supporting salts was utilized to ensure the desirable electrochemical performances caused by the ionization−hydrolysis equilibrium between acid and supporting salt. Initially, the acid solution successfully eliminated the side reactions caused by carbon dioxide and the supporting salt enhanced the conductivity of catholyte. Therefore, as shown in Figure 4a,b, both the cells using 0.1 M HAc + 0.1 M NaAc and 0.1 M H_3PO_4 + 0.1 M Na_2SO_4 as catholyte showed a higher discharge voltage than their alkaline-based hybrid sodium−air cell counterparts.[4,9] Consequently, the improved discharge voltage compared to that of the alkaline-based hybrid sodium−air cells significantly contributes to a higher power density, which will be discussed later. To analyze the influence of supporting salts on the cell voltage, different concentrations of NaAc and Na_2SO_4 were added into HAc and H_3PO_4, respectively. As shown in Figure 4a,b, similar trends were observed using the two aqueous electrolytes. The discharge voltage decreased greatly with an increase of support salt concentration. This is due to the limitation of the four-electron reaction of cells ($O_2 + 2H_2O + 4e^- = 4OH^-$) on increasing the concentration of support salts. This result may seem counterintuitive, since H_3PO_4 and Na_2SO_4 are almost completely ionized in the catholyte, which may lead us to believe that the discharge voltage will increase due to the increased presence of high ionic conductivity species. The inset is the supporting salt concentration dependence of discharge voltage in hybrid sodium−air cell, which indicates that high concentration of supporting salt limits the original four-electron transfer reaction due to the lower solubility of oxygen in aqueous electrolyte, thus decreasing the discharge voltage of the cells.[8] Compared with 0.1 M HAc, 0.1 M H_3PO_4 exhibited relatively higher discharge voltages at the same supporting salt concentrations, which is due to the higher ionic conductivity of the H_3PO_4 and Na_2SO_4 mixture.

Figure 5 shows the discharge−charge voltage curves of hybrid sodium−air cells when the current density is 0.13 mA cm^{-2}. The cell using 0.1 M H_3PO_4 + 0.1 M Na_2SO_4 as catholyte indicated a slightly higher voltage plateau (3.4 V) compared to that of the other one. This is mainly because 0.1 M H_3PO_4 + 0.1 M Na_2SO_4 solution has relatively high ionic conductivity. However, high H^+ concentration limits the catalytic performance toward the oxygen evolution reaction (OER), thus leading to a slightly higher charge voltage compared to that of the cell with 0.1 M HAc + 0.1 M NaAc. Therefore, the same voltage gap (0.3 V) was observed in these two cells, which corresponds to high round-trip efficiency of 92%. Some data about voltage gap of alkaline

DOI: 10.1021/acsami.8b04278
ACS Appl. Mater. Interfaces XXXX, XXX, XXX−XXX

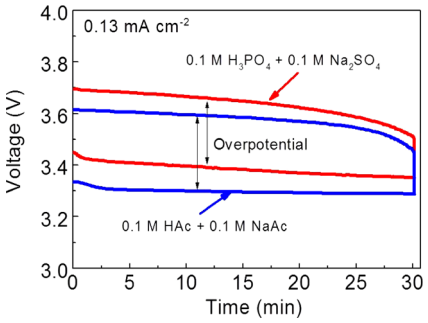

Figure 5. Discharge−charge voltage curves of hybrid sodium−air cells at a current density of 0.13 mA cm^{-2}.

metal−air cells are shown in Table 2, which indicates the cell system has a significant effect on the round-trip efficiency when the same Pt/C was used as catalyst. Obviously, because of the higher activity of metallic sodium than that of lithium, hybrid sodium−air cells indicated a lower voltage plateau gap than that of hybrid lithium−air cells.[4,8,9,27−29] In addition, the round-trip efficiency is greatly improved due to the relatively lower activation energy for combining sodium with O_2 and H_2O.[30] At last, the high ionic conductivity of NASICON significantly decreased the voltage plateau gap, thus improving the efficiency.[4] Ceramic separators with high ionic conductivity provide many Na^+ transmission channels and desirable grain-boundary structure, thus improving Na^+ diffusion.[4,8] Furthermore, the acid solution effectively inhibits detrimental side reactions and increases the round-trip efficiency.

Recently, Kim et al. reported that a larger voltage gap was obtained when utilizing neutral catholytes compared with the acidic and alkaline counterparts; this mainly corresponds to a significant lack of H^+ or OH^-, which greatly limited the cell reactions.[25] This indicates that the overpotential and round-trip efficiency can also be enhanced by optimizing the catholyte system rather than selecting appropriate catalysts. It can be clearly seen that the average round-trip efficiency of acid-based hybrid sodium−air cells is higher than that of cells containing an alkaline catholyte. Because of higher discharge and charge voltage, even if the same voltage gap was obtained by both acidic and alkaline catholytes, acid-based hybrid sodium−air cells still exhibit slightly higher round-trip efficiency.

Figure 6a shows the EIS analysis of the hybrid sodium−air cells with the open circuit condition at 20 °C. In the circuit, the ohmic resistance (R_e) (the intercept of semicircle on the real axis) is indicated in the high frequency, which is contributed by the bulk resistance of NASICON and the two liquid electrolytes. The interfacial resistances (R_i) are reflected by the large semicircle in the high-frequency range, which is explained by the grain-boundary resistance of NASICON and the interfaces' resistance between the solid and liquid electrolytes. In the middle-frequency region, the smaller semicircle can be noted, corresponding to the resistance (R_s) of a NASICON interphase on the sodium surface and the charge-transfer resistance (R_{ct}) in an air electrode. The related capacitances are reflected by the constant-phase elements (CPE_i, CPE_s, and CPE_{ct}). The finite-length Warburg element (Z_w) is demonstrated in the lowest frequency range, which arises from a diffusion process in the air electrode. From the fitted EIS data (solid plots), the total resistances of 240.29 and 343.74 Ω were obtained for cell i and cell ii, respectively. It is obvious that cell ii displayed larger resistance than that of cell i, especially for R_e and R_i. Although NASICON shows good stability in HAc solution, the mixture of HAc and NaAc show a lower ionic conductivity due to incomplete ionization, causing a lower discharge voltage.[26,27] In addition, cell reaction changed from 4 to 1 because just one H^+ of the HAc is consumed in aqueous electrolyte during discharging.[26,27] Conversely, because the protons of phosphoric acid and Na_2SO_4 are nearly ionized, the 0.1 M H_3PO_4 + 0.1 M Na_2SO_4 catholyte exhibits superior ionic conductivity. More importantly, the three protons of phosphoric acid enable a larger cell energy density, ensuring long-term stability of cells.[27]

Figure 6b shows the current−voltage profiles of the hybrid sodium−air cells at a scan rate of 5 mV s^{-1} with a potentiostat. A maximum power density of 19.6 and 17.3 mW cm^{-2} was obtained for cell i and cell ii, respectively, which is better than that of the acidic hybrid lithium−air fuel cell developed by Li et al.[27,33] Furthermore, the cell with 0.1 M H_3PO_4 + 0.1 M Na_2SO_4 exhibits a higher maximum power density than that of the cell with 0.1 M HAc + 0.1 M NaAc because of the lower internal resistance of the cell. The activation polarization of catalyst toward ORR leads to a sharp decrease initially.[26] The almost linear polarization curve at high current density indicated that R_e and R_i are dominant.[33] Therefore, the hybrid sodium−air cell possesses much higher working voltage and power density,

Table 2. Summary of the Discharge Behaviors of Hybrid Alkali Metal−Air Cells with Pt/C Catalysts

system	catalysts	current density/catholyte	voltage gap (V)	round-trip efficiency (%)	ref
Li−air (acidic)	Pt	0.5 mA cm^{-2}/HOAc−H_2O−LiOAc	0.70	83.3	26
Li−air (alkaline)	Pt/C (50%)	0.05 mA cm^{-2}/0.01 M $LiClO_4$	0.7	82.5	31
Li−air (neutral)	Pt/C (50%)	12.5 mA g^{-1}	0.4	89.3	32
Li−air (acidic)	Pt	0.5 mA cm^{-2}/0.1 M H_3PO_4 + 1 M LiH_2PO_4	0.9	76.1	33
Li−air (acidic)	IrO_2 and Pt/C	0.5 mA cm^{-2}/0.1 M H_3PO_4 + 1 M Li_2SO_4	0.9	76.2	27
Li−air (alkaline)	Pt/C + NCONF	0.5 mA cm^{-2}/0.5 LiOH + 1 M $LiNO_3$	0.7	81.6	34
Li−air (alkaline)	Pt/C + NCONF@Ni	0.5 mA cm^{-2}/0.5 LiOH + 1 M $LiNO_3$	0.7	80.5	34
Na−air (alkaline)	Pt/C (50%)	0.1 mA cm^{-2}/0.1 M NaOH	0.53	84.3	17
Na−air (alkaline)	Pt/C (50%)	60 mA g^{-1}/0.1 M NaOH	0.18	94.3	35
Na−air (alkaline)	Pt/C (50%)	0.01 mA cm^{-2}/0.1 M NaOH	0.61	82.8	18
Na−air (alkaline)	Pt/C (50%)	0.13 mA cm^{-2}/1 M NaOH	0.62	81.5	22
Na−air (acidic)	Pt/C-loaded HCF	0.1 mA cm^{-2}/0.1 M CA + 1 M $NaNO_3$	0.46	87.9	25
Na−air (acidic)	Pt/C−IrO_2 loaded HCF	0.1 mA cm^{-2}/0.1 M CA + 1 M $NaNO_3$	0.36	90.2	25
Na−air (acidic)	Pt/C (40%)	0.1 mA cm^{-2}/0.1 M H_3PO_4 + 0.1 M Na_2SO_4	0.30	92.0	present work
Na−air (acidic)	Pt/C (40%)	0.1 mA cm^{-2}/0.1 M HAc + 0.1 M NaAc	0.30	91.7	present work

DOI: 10.1021/acsami.8b04278
ACS Appl. Mater. Interfaces XXXX, XXX, XXX−XXX

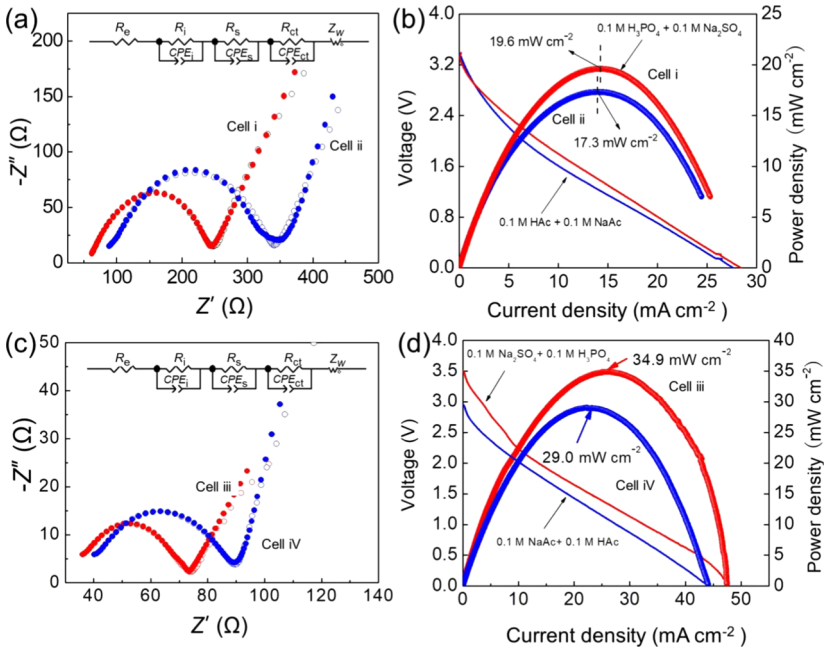

Figure 6. Electrochemical performances of the acidic electrolyte sodium−air cells: (a) EIS analysis of cells at 20 °C (cells i and ii correspond to catholytes with 0.1 M H_3PO_4 + 0.1 M Na_2SO_4 and 0.1 M HAc + 0.1 M NaAc, respectively). The inset is the equivalent circuit for fitting the measured data (open circle dots), and the solid colored dots indicate the fitted spectra; (b) Current−voltage and areal power density−voltage of cells at 20 °C; (c) EIS of cells at 30 °C (cells iii and iv correspond to catholytes with 0.1 M H_3PO_4 + 0.1 M Na_2SO_4 and 0.1 M HAc + 0.1 M NaAc, respectively); (d) Current−voltage and areal power density−voltage characteristics of cells at 30 °C.

Table 3. Elemental Resistances (R_e, R_i, R_s, R_{ct}, and Z_w) in the Equivalent Circuits Estimated in Four Cells

cell no.	catholyte	R_e (Ω)	R_i (Ω)	R_s (Ω)	R_{ct} (Ω)	Z_w (Ω)
i	0.1 M H_3PO_4 + 0.1 M Na_2SO_4, 20 °C	54.57	157.50	14.98	12.95	0.29
ii	0.1 M HAc + 0.1 M NaAc, 20 °C	78.19	209.8	32.91	22.54	0.30
iii	0.1 M H_3PO_4 + 0.1 M Na_2SO_4, 30 °C	31.30	32.95	5.05	3.36	0.19
iv	0.1 M HAc + 0.1 M NaAc, 30 °C	33.95	48.98	5.81	5.19	0.22

which are even superior to those of Li−air cells with similar structure.[33,36−38]

To explore the dependence of temperature on power density, cells were tested at 30 °C. It was found that increasing temperature significantly reduces the internal resistance of the cells. As shown in Figure 6c and Table 3, the two largest reductions of impedance lie in R_e and R_i by increasing temperature.[4,9] R_e decreased by around 50% when the temperature was increased to 30 °C; this is because of the improvement of ionic conductivity in the liquid electrolyte and NASICON at higher temperature.[4] Similarly, this also occurred in the resistance of the interfaces; R_i decreased from 209.8 to 48.98 Ω and 157.50 to 32.95 Ω for cell iii and cell iv, respectively. This effect can be attributed to the decrement in R_e and R_i.[44] First, the viscosity of the aprotic electrolyte decreases at elevated temperature and enhances the contact between the aprotic electrolyte and NASICON, thus accelerating Na^+ diffusion in the interface between NASICON and liquid electrolyte. In addition, the grain-boundary structural transition of the ceramic separator provides a mass of Na^+ transmission channels and promotes Na^+ diffusion.[39] R_s and R_{ct} also experienced the same trend; increment of temperature not only contributes to a more favorable composition and morphology of SEI, but also improves the catalytic performance.[40] Therefore, decrements of R_s and R_{ct} components greatly contributed to the power density. As shown in Figure 6d, the maximum power densities of 34.9 and 29.0 mW cm^{-2} were observed for cell iii and cell iv, respectively. In addition, increasing the ionic conductivity of NASICON and exploring more effective catalysts for OER and ORR contribute in enhancing the power density of a cell definitely. Table 4 shows the maximum power densities of lithium−air and sodium−air cells, indicating high maximum output power density of acid-based hybrid sodium−air cells.

The discharge capacities of the cells were calculated by integrating discharge curves, as shown in Figure 7. According to the cell reaction, active materials of Na and H^+ were used to calculate the cell capacities.[4] The capacities at the terminal points for the acidic hybrid sodium−air cells with different aqueous electrolytes were 896 and 881 mAh g^{-1}, respectively, which is 80 and 79% of the theoretical values. The loss of capacities can be explained by the following reasons: First, the losses are mainly ascribed to the oxidation of Na during cell assembly or operation caused by leakage of O_2 or H_2O into the anode compartment.[4,9] Because the amount of Na in each test was quite small, surface oxidation would have a marked effect on the apparent capacity.[4,9] Another possible contribution is the side reaction of Na with the organic electrolyte or NASICON separator.[4,9] In addition, the loss of cell capacity may be influenced by the NASICON separator and the accumulation of Na^+ in the transport channels.[4] Further investigation is required to clarify the origin of these losses. The practical energy density is an important parameter for real application of the fabricated hybrid sodium−air cells and is calculated to be 2329 Wh kg^{-1} on

DOI: 10.1021/acsami.8b04278
ACS Appl. Mater. Interfaces XXXX, XXX, XXX−XXX

Table 4. Areal Power Densities in Alkali Metal−Air Cells

cell	maximum power density (mW cm^{-2})	temperature (°C)	ref
hybrid Li−air (alkaline)	16	25	41
hybrid Li−air (acidic)	11.9	25	33
hybrid Li−air (acidic)	19	30	42
hybrid Li−air (acidic)	30	40	42
hybrid Na−air (alkaline)	5.0	50	8
hybrid Na−air (alkaline)	10.0		8
hybrid Na−air (alkaline)	21	25	9
hybrid Na−air (alkaline)	27.6	50	4
hybrid Na−air (alkaline)	26.3	70	4
hybrid Na−air (alkaline)	12.4	25	16
hybrid Na−air (acidic)	5	25	25
hybrid Na−air (acidic)	29.0	30	present work
hybrid Na−air (acidic)	34.9	30	present work

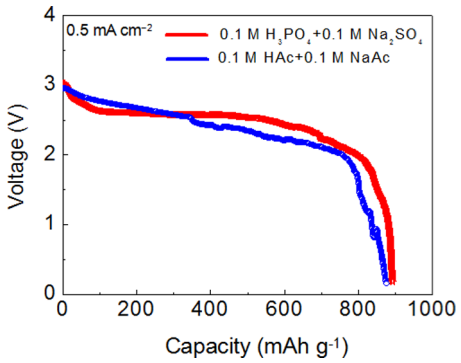

Figure 7. Discharge curves of hybrid sodium−air cells at a current density of 0.5 mA cm^{-2}.

the basis of active materials, which can satisfy the requirement of long-range electric vehicles.[40,43−48]

To evaluate the rechargeability, cells were tested for 30 cycles at a current density of 0.13 mA cm^{-2}. As shown in Figure 8, the

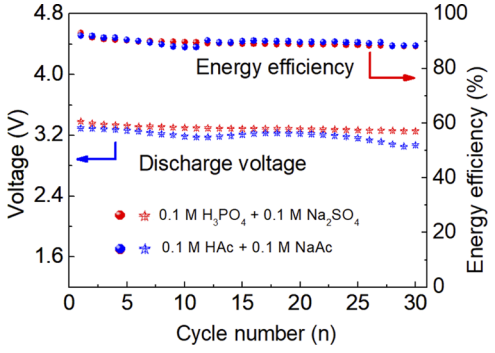

Figure 8. Energy efficiency and discharge voltage of hybrid sodium−air cells at a current density of 0.13 mA cm^{-2}.

cell with 0.1 M H_3PO_4 + 0.1 M Na_2SO_4 displayed a slightly higher discharge voltage than that of the one containing 0.1 M HAc + 0.1 M NaAc due to the higher ion conductivity of the catholyte, which leads to a higher power density. However, a similar voltage plateau gap was observed during cycling along with an initial energy efficiency of 92%, which indicates superior discharge behaviors of hybrid sodium−air cells with acid electrolytes. High average energy efficiency of around 90% was observed during the entire cycling period. On one hand, the performance can be ascribed to the highly efficient catalytic behavior of Pt/C catalyst; high conductivity of carbon and amounts of active sites both promote the direct reduction of oxygen and hydroxyl and greatly decrease the voltage gap while enhancing the energy efficiency of the cells.[17] On the other hand, the reversible change of catholyte provides a buffering effect during the discharge process, which also contributes to the good rechargeability and electrochemical stability.[27] However, the voltage gap slightly increased by around 0.1 V after 30 cycles due to the unavoidable evaporation of aqueous electrolyte at 30 °C.[4,9] As investigated previously, the discharge voltage of the cell decreases with increasing concentration of aqueous electrolyte, which contributes to the increase of voltage gap.[4,9] Therefore, to solve the concentration change of aqueous electrolyte, a circulation system was proposed to maintain the aqueous electrolyte flow. Furthermore, the poor density of deposited Na affected the cell performances, which is actually common in hybrid metal−air batteries.

The morphological and structural changes of the NASICON and catalyst after discharge cycling were investigated by scanning electron microscopy (SEM) and XRD (Figures S1−S3). There is no evidence to prove the new physical interface formation on the NASICON. In addition, SEM images of catalysts before and after cycling are depicted in Figure S4; no significant difference was obtained in the morphology of catalytic electrode, which indicates an acceptable stability. The Pt/C cell features a direct four-electron transfer pathway.[25,49,50]

CONCLUSIONS

A novel high-energy-density hybrid sodium−air cell with acid electrolyte was successfully fabricated. The hybrid sodium−air cell not only offered a higher standard cell voltage of 3.94 V, theoretical specific capacity of 1121 mAh g^{-1}, and energy density of 4418 Wh kg^{-1} but also successfully eliminated the side reaction caused by carbon dioxide. Generally, strong acids are undesirable for the hybrid metal−air cells due to the significant corrosion of NASICON. Therefore, weak acids such as HAc and H_3PO_4 were chosen as candidates. First, the effects of supporting salts on the discharge behaviors of the hybrid sodium−air cell were systematically investigated; it was found that higher concentration of supporting salts leads to a lower discharge voltage due to the decreased solubility of oxygen. Subsequently, electrochemical performances of cells with 0.1 M H_3PO_4 + 0.1 M Na_2SO_4 and 0.1 M HAc + 0.1 M NaAc were compared and the buffering effect of 0.1 M H_3PO_4 + 0.1 M Na_2SO_4 solution with a three-proton system lead to stable and long discharge cell behaviors. In addition, the hybrid sodium−air cell with acidic electrolyte cell demonstrated a maximum output power density of 34.9 mW cm^{-2} at 30 °C by using 0.1 M H_3PO_4 + 0.1 M Na_2SO_4 as the catholyte. Furthermore, the capacities of hybrid Na−air cells with 0.1 M H_3PO_4 + 0.1 M Na_2SO_4 and 0.1 M HAc + 0.1 M NaAc as catholyte were 896 and 881 mAh g^{-1}, respectively. More importantly, the fabricated acidic-based hybrid sodium−air cells delivered a low voltage gap of 0.3 V

DOI: 10.1021/acsami.8b04278
ACS Appl. Mater. Interfaces XXXX, XXX, XXX−XXX

and the round-trip energy efficiency reached up to 90% during 30 cycles. Therefore, acid-based hybrid sodium−air cells are proved to be excellent cost-effective energy storage technologies.

■ ASSOCIATED CONTENT

Supporting Information

The Supporting Information is available free of charge on the ACS Publications website at DOI: 10.1021/acsami.8b04278.

XRD patterns, SEM images, and energy-dispersive spectrum of NASICON before and after cycling; SEM images of catalysts before and after cycling (PDF)

■ AUTHOR INFORMATION

Corresponding Author

*E-mail: liangfeng@kmust.edu.cn. Tel/Fax: +86-871-6510720. Xuefu Road 253, Kunming 650093, Yunnan, China.

ORCID

Feng Liang: 0000-0003-4718-652X
Kunfeng Chen: 0000-0001-9253-1885
Katsuro Hayashi: 0000-0002-4413-6511
Hossein Yadegari: 0000-0002-2572-182X
Xueliang Sun: 0000-0003-2881-8237

Author Contributions

[▽]Y.K. and F.S. are contributed equally to this article.

Notes

The authors declare no competing financial interest.

■ ACKNOWLEDGMENTS

This work was financially supported by the National Natural Science Foundation of China (51704136 and 11765010), the Open Project of the State Key Laboratory of Rare Earth Resource Utilization (RERU2016019), and the Applied Basic Research Programs of Yunnan Provincial Science and Technology Department (2016FB087). This research was supported by Natural Sciences and Engineering Research Council of Canada, Canada Research Chair Program, and the University of Western Ontario.

■ REFERENCES

(1) Kim, H.; Kim, H.; Ding, Z.; Lee, M. H.; Lim, K.; Yoon, G.; Kang, K. Recent Progress in Electrode Materials for Sodium-Ion Batteries. *Adv. Energy Mater.* **2016**, *6*, No. 1600943.

(2) Yu, J.; Hu, Y. S.; Pan, F.; Zhang, Z. Z.; Wang, Q.; Li, H.; Huang, X. J.; Chen, L. Q. A Class of Liquid Anode for Rechargeable Batteries with Ultralong Cycle Life. *Nat. Commun.* **2017**, *8*, No. 14629.

(3) Kim, J. K.; Mueller, F.; Kim, H.; Jeong, S.; Park, J. S.; Passerini, S.; Kim, Y. Eco-friendly Energy Storage System: Seawater and Ionic Liquid Electrolyte. *ChemSusChem* **2016**, *9*, 42−49.

(4) Kang, Y.; Liang, F.; Hayashi, K. Hybrid Sodium-Air Cell with Na[FSA-C_2C_1im][FSA] Ionic Liquid Electrolyte. *Electrochim. Acta* **2016**, *218*, 119−124.

(5) Kim, S. K.; Lim, E.; Kim, S.; Jo, C.; Chun, J. Y.; Lee, J. General Synthesis of N-doped Macroporous Graphene-Encapsulated Mesoporous Metal Oxides and Their Application as New Anode Materials for Sodium-Ion Hybrid Supercapacitors. *Adv. Funct. Mater.* **2017**, *27*, No. 1603921.

(6) Kundu, D.; Talaie, E.; Duffort, V.; Nazar, L. F. The Emerging Chemistry of Sodium Ion Batteries for Electrochemical Energy Storage. *Angew. Chem., Int. Ed.* **2015**, *54*, 3431−3448.

(7) Xiang, X.; Zhang, K.; Chen, J. Recent Advanced and Prospects of Cathode Materials for Sodium-Ion Batteries. *Adv. Mater.* **2015**, *27*, 5343−5364.

(8) Hayashi, K.; Shima, K.; Sugiyama, F. A Mixed Aqueous/Aprotic Sodium/Air Cell Using a NASICON Ceramic Separator. *J. Electrochem. Soc.* **2013**, *160*, A1467−A1472.

(9) Liang, F.; Hayashi, K. A High-Energy-Density Mixed-Aprotic-Aqueous Sodium-Air Cell with a Ceramic Separator and a Porous Carbon Electrode. *J. Electrochem. Soc.* **2015**, *162*, A1215−A1219.

(10) Yadegari, H.; Sun, Q.; Sun, X. L. Sodium-Oxygen Batteries: A Comparative Review from Chemical and Electrochemical Fundamentals to Future Perspective. *Adv. Mater.* **2016**, *28*, 7065−7093.

(11) Landa-Medrano, I.; Li, C. M.; Ortiz-Vitoriano, N.; Ruiz de Larramendi, I.; Carrasco, J.; Rojo, T. Sodium-Oxygen Battery: Steps Toward Reality. *J. Phys. Chem. Lett.* **2016**, *7*, 1161−1166.

(12) Ortiz-Vitoriano, N.; Batcho, T. P.; Kwabi, D. G.; Han, B.; Pour, N.; Yao, K. P. C.; Thompson, C. V.; Shao-Horn, Y. Rate-Dependent Nucleation and Growth of NaO_2 in Na-O_2 Batteries. *J. Phys. Chem. Lett.* **2015**, *6*, 2636−2646.

(13) Kang, S.; Mo, Y.; Ong, S. P.; Ceder, G. Nanoscale Stabilization of Sodium Oxides: Implications for Na-O_2 Batteries. *Nano Lett.* **2014**, *14*, 1016−1020.

(14) Lee, B. J.; Seo, D.-H.; Lim, H.-D.; Park, I.; Park, K.-Y.; Kim, J.; Kang, K. First-Principles Study of the Reaction Mechanism in Sodium-Oxygen Batteries. *Chem. Mater.* **2014**, *26*, 1048−1055.

(15) Yadegari, H.; Li, Y.; Banis, M. N.; Li, X.; Wang, B.; Sun, Q.; Li, R.; Sham, T.-K.; Cui, X.; Sun, X. On Rechargeability and Reaction Kinetics of Sodium-Air Batteries. *Energy Environ. Sci.* **2014**, *7*, 3747−3757.

(16) Hashimoto, T.; Hayashi, K. Aqueous and Nonaqueous Sodium-Air Cells with Nanoporous Gold Cathode. *Electrochim. Acta* **2015**, *182*, 809−814.

(17) Sahgong, S.; Senthilkumar, S. T.; Kim, K.; Hwang, S. M.; Kim, Y. Rechargeable Aqueous Na-Air Batteries: Highly Improved Voltage Efficiency by Use of Catalysts. *Electrochem. Commun.* **2015**, *61*, 53−56.

(18) Senthilkumar, B.; Khan, Z.; Park, S.; Seo, I.; Ko, H.; Kim, Y. Exploration of Cobalt Phosphate as A Potential Catalyst for Rechargeable Aqueous Sodium-Air Battery. *J. Power Sources* **2016**, *311*, 29−34.

(19) Li, Y.; Yadegari, H.; Li, X.; Banis, M. N.; Li, R.; Sun, X. Superior Catalytic Activity of Nitrogen-Doped Graphene Cathodes for High Energy Capacity Sodium-Air Batteries. *Chem. Commun.* **2013**, *49*, 11731−11733.

(20) Jian, Z.; Chen, Y.; Li, F.; Zhang, T.; Liu, C.; Zhou, H. High Capacity Na-O_2 Batteries with Carbon Nanotube Paper as Binder-Free Air Cathode. *J. Power Sources* **2014**, *251*, 466−469.

(21) Liu, W.; Sun, Q.; Yang, Y.; Xie, J. Y.; Fu, Z. W. An Enhanced Electrochemical Performance of a Sodium-Air Battery with Graphene Nanosheets as Air Electrode Catalysts. *Chem. Commun.* **2013**, *49*, 1951−1953.

(22) Kang, Y.; Zou, D.; Zhang, J. Y.; Liang, F.; Hayashi, K.; Wang, H.; Xue, D. F.; Chen, K. F.; Adair, K. R.; Sun, X. L. Dual−phase Spinel $MnCo_2O_4$ Nanocrystals with Nitrogen-doped Reduced Graphene Oxide as potential Catalyst for Hybrid Na−Air Batteries. *Electrochim. Acta* **2017**, *244*, 222−229.

(23) Liang, F.; Watanabe, T.; Hayashi, K.; Yao, Y. C.; Ma, W. H.; Yang, B.; Dai, Y. N. Liquid Exfoliation Graphene Sheets as Catalysts for Hybrid Sodium-Air Cells. *Mater. Lett.* **2017**, *187*, 32−35.

(24) Thotiyl, M. M. O.; Freunberger, S. A.; Peng, Z.; Chen, Y.; Liu, Z.; Bruce, P. G. A Stable Cathode for the Aprotic Li−O_2 Battery. *Nat. Mater.* **2013**, *12*, 1050−1056.

(25) Hwang, S. M.; Go, W.; Yu, H.; Kim, Y. Hybrid Na-Air Flow Batteries Using an Acidic Catholyte: Effect of the Catholyte pH on the Cell Performance. *J. Mater. Chem. A* **2017**, *5*, 11592−11600.

(26) Zhang, T.; Imanishi, N.; Shimonishi, Y.; Hirano, A.; Takeda, Y.; Yamamotoa, O.; Sammesb, N. A Novel High Energy Density Rechargeable Lithium/Air Cell. *Chem. Commun.* **2010**, *46*, 1661−1663.

(27) Li, L. J.; Zhao, X. S.; Fu, Y. Z.; Manthiram, A. Polyprotic Aid Catholyte for High Capacity Dual−Electrolyte Li−air Cells. *Phys. Chem. Chem. Phys.* **2012**, *14*, 12737−12740.

(28) Manthiram, A.; Li, L. J. Hybrid and Aqueous Lithium−Air Batteries. *Adv. Energy Mater.* **2015**, *5*, No. 1401302.

DOI: 10.1021/acsami.8b04278
ACS Appl. Mater. Interfaces XXXX, XXX, XXX−XXX

(29) Fuentes, R. O.; Figueiredo, F.; Marques, F. M. B.; Franco, J. I. Reaction of NASICON with Water. *Solid State Ionics* **2001**, *139*, 309−314.
(30) Krishnamurthy, D.; Hansen, H. A.; Viswanathan, V. Universality in Nonaqueous Alkali Oxygen Reduction on Metal Surfaces: Implications for Li-O_2 and Na-O_2 Batteries. *ACS Energy Lett.* **2016**, *1*, 162−168.
(31) He, H.; Niu, W.; Asl, N. M.; Salim, J.; Chen, R.; Kim, Y. Effects of Aqueous Electrolytes on the Voltage Behaviors of Rechargeable Li-Air Batteries. *Electrochim. Acta* **2012**, *67*, 87−94.
(32) Kim, J. K.; Yang, W.; Salim, J.; Ma, C.; Sun, C. W.; L, J. Q.; Kim, Y. Li-water Battery with Oxygen Dissolved in Water as a Cathode. *J. Electrochem. Soc.* **2014**, *161*, A285−A289.
(33) Li, L.; Zhao, X.; Manthiram, A. A Dual-Electrolyte Rechargeable Li-Air Battery with Phosphate Buffer Catholyte. *Chem. Commun.* **2012**, *14*, 78−81.
(34) Li, L. J.; Chai, S. H.; Dai, S.; Mamthiram, A. Advanced Hybrid Li-Air Batteries with High-Performance Mesoporous Nanocatalysts. *Energy Environ. Sci.* **2014**, *7*, 2630−2636.
(35) Cheon, J. Y.; Kim, K.; Sa, Y. J.; Sahgong, S. H.; Hong, Y.; Woo, J.; Yim, S. D.; Jeong, H. Y.; Kim, Y.; Joo, S. H. Graphitic Nanoshell/Mesoporous Carbon Nanohybrids as Highly Efficient and Stable Bifunctional Oxygen Electrocatalysts for Reachargeable Aqueous Na-Air Batteries. *Adv. Energy Mater.* **2016**, *6*, No. 1501794.
(36) Hartmann, P.; Bender, C. L.; Sann, J.; Dürr, A. K.; Jansen, M.; Janek, J.; Adelhelm, P. A Comprehensive Study on the Cell Chemistry of the Sodium Superoxide (NaO_2) cell. *Phys. Chem. Chem. Phys.* **2013**, *15*, 11661−11672.
(37) Bender, C. L.; Jache, B.; Adelhelm, P.; Janek, J. Sodiated carbon: A Reversible Anode for the Sodium-Oxygen Cell and Route for the Chemical Synthesis of Sodium Superoxide (NaO_2). *J. Mater. Chem. A* **2015**, *3*, 20633−20641.
(38) Liu, T.; Leskes, M.; Yu, W.; Moore, A. J.; Zhou, L.; Bayley, P. M.; Kim, G.; Grey, C. P. Cycling Li-O_2 Cells via LiOH Formation and Decomposition. *Science* **2015**, *350*, 530−533.
(39) Lee, S. B.; Lee, J. H.; Cho, P. S.; Kim, D. Y.; Sigle, W.; Phillipp, F. High-Temperature Resistance Anomaly at a Strontium Titanate Grain Boundary and Its Correlation with the Grain-Boundary Faceting-Defaceting Transition. *Adv. Mater.* **2007**, *19*, 391−395.
(40) Byrne, N.; Howlett, P. C.; MacFarlane, D. R.; Forsyth, M. The Zwitterion Effect in Ionic Liquids: Towards Practical Rechargeable Lithium-Metal Batteries. *Adv. Mater.* **2005**, *17*, 2497−2501.
(41) Wang, Y.; Zhou, H. S. A Lithium-Air Battery with a Potential to Continuously Reduce O_2 From Air for Delivering Energy. *J. Power Sources* **2010**, *195*, 358−361.
(42) Li, L. J.; Manthiram, A. Hybrid Lithium−Air Batteries: Influence of Catalyst, Temperature, and Solid-Electrolyte Conductivity on the Efficiency and Power Density. *J. Mater. Chem. A* **2013**, *1*, 5121−5127.
(43) Jian, Z. L.; Chen, Y.; Li, F. J.; Zhang, T.; Liu, C.; Zhou, H. S. High Capacity Na-O_2 Cells with Carbon Nanotube Paper as Binder-Free Air Cathode. *J. Power Sources* **2014**, *251*, 466−469.
(44) Li, Y. L.; Yadegari, H.; Li, X. F.; Banis, M. N.; Li, R. Y.; Sun, X. L. Superior Catalytic Activity of Nitrogen−Doped Graphene Cathodes for High Energy Capacity Sodium-Air Cells. *Chem. Commun.* **2013**, *49*, 11731−11733.
(45) Sun, Q.; Yadegari, H.; Banis, M. N.; Liu, J.; Xiao, B. W.; Wang, B. Q.; Lawes, S.; Li, X.; Li, R. Y.; Sun, X. L. Self-Stacked Nitrogen-Doped Carbon Nanotubes as Long-Life Air Electrode for Sodium-Air Cells: Elucidating the Evolution of Discharge Product Morphology. *Nano Energy* **2015**, *12*, 698−708.
(46) Tarascon, J. M.; Armand, M. Issues and Challenges Facing Rechargeable Lithium Cells. *Nature* **2001**, *414*, 359−367.
(47) Goodenough, J. B.; Park, K. S. The Li-Ion Rechargeable Cell: A Perspective. *J. Am. Chem. Soc.* **2013**, *135*, 1167−1176.
(48) Mizushima, K.; Jones, P. C.; Wiseman, P. J.; Goodenough, J. B. Li_xCoO_2 ($0 < x < 1$): A New Cathode Material for Batteries of High Energy Density. *Solid State Ionics* **1981**, *3*−*4*, 171−174.
(49) He, P.; Zhang, T.; Jiang, J.; Zhou, H. S. Lithium-Air Batteries with Hybrid Electrolytes. *J. Phys. Chem. Lett.* **2016**, *7*, 1267−1280.
(50) Kinoshita, K. Electrochemical Oxygen Technology. *The Electrochemical Society*; Wiley: Chichester, 1992.

DOI: 10.1021/acsami.8b04278
ACS Appl. Mater. Interfaces XXXX, XXX, XXX−XXX